Available online at www.sciencedirect.com

ScienceDirect

IFAC PapersOnline CONFERENCE PAPER ARCHIVE

IFAC PapersOnLine 55-18 (2022) 50–55

First passage times as a measure of hysteresis in stochastic gene regulatory circuits ⋆

Manuel Pájaro * **Irene Otero-Muras** ** **Antonio A. Alonso** ***

* *Department of Mathematics and CITIC research center, University of A Coruña, Campus Elviña s/n, 15071 A Coruña (e-mail: manuel.pajaro@udc.es)*

** *Computational Synthetic Biology Group, I2SYSBIO Institute for Integrative Systems Biology (CSIC-UV), 46980 València*

*** *Bioprocess Engineering Group, IIM-CSIC, Spanish National Council for Scientific Research, 36208 Vigo*

Abstract: In the context of phenotype switching and cell fate determination, numerous experimental studies report hysteresis, despite the fact that the (forward) Chemical Master Equation governing the inherently stochastic underlying gene regulatory networks has a unique steady state (precluding memory effects and hysteresis). In previous works, we demonstrate that hysteresis is a transient phenomenon in systems far from the thermodynamic limit, using the convergence rates of the partial integro-differential equation associated to the forward master equation governing the stochastic process. Here, we make use of the backward master equation to quantify hysteresis and irreversibility based on First Passage Times.

First, we derive the backward master equation for a gene regulatory network with protein production in bursts. Solving this equation, we obtain the probability distributions of the first times to reach some fixed final state from one starting state. The mean first passage time provides a measure to quantify how hysteresis and irreversibility in gene regulation at the single cell level are transient effects that vanish at steady state. In addition, we provide a theoretical basis that reconciles phenotype coexistence and prevalence far from the thermodynamic limit. In fact, we substitute the notion of pseudo-potential (the so-called Waddington landscape) by a time evolving landscape built upon the Chemical Master Equation (CME) in which phenotypes, rather than prevail, persist with different intensities.

Keywords: Gene regulation, cell decision-making, hysteresis, Chemical Master Equation, stochastic dynamics, bistability, First Passage Times.

1. INTRODUCTION

Hysteresis is a well known phenomenon in nonlinear dynamics. It occurs when a graded stimulus produces a discontinuous (ON-OFF) response in the measured steady state of the system upon a given threshold and, in addition, the system switches on and off for two different thresholds of the signal. In this way, the system's steady state follows a different path depending on whether the input signal is increasing or decreasing. This type of ON-OFF response is a widespread mechanism in cell regulatory systems underlying phenotype switching and cell determination (Veening et al., 2008). Hysteresis ensures a reliable cell decision in response to stimuli, as it enables the acquired phenotype to persist long upon withdrawal of the signal (Celià-Terrassa et al., 2018). In this context, both reversible and irreversible scenarios (Xiong and Ferrell, 2012; Wang et al., 2009; Ferrell, 2012; Wu et al., 2013) have been experimentally observed (reversibility must be understood here as the capacity of individual cells to switch back in absence of external signals (Gupta et al., 2011)).

The dynamics of a gene regulatory network (GRN) is inherently stochastic, being the time evolution of the probability distribution of the system state governed by a Chemical Master Equation (CME). The steady state solution of the CME is unique, and therefore independent on the initial state of the system (Van Kampen, 2007). Therefore, stochastic gene regulatory processes are in principle incompatible with memory effects or hysteresis. However, in numerous studies, hysteresis has been found in gene regulatory networks subject to significant levels of stochasticity (Ozbudak et al., 2008; Thomas et al., 2014; Gnügge et al., 2016; Hsu et al., 2016).

Pájaro et al. (2019) resolved this apparent discrepancy demonstrating that, for stochastic gene regulatory networks, hysteresis and irreversibility at the single cell level are transient effects that vanish at the steady state. To this aim, the authors computed the convergence rates of an accurate approximation of the CME by a Partial-Integro Differential Equation (PIDE) (Friedman et al.,

⋆ MP acknowledges support from grant FJC2019-041397-I funded by MCIN/AEI/ 10.13039/501100011033. IOM acknowledges support from GAIN Oportunius Grant from Xunta de Galicia.

10.1016/j.ifacol.2022.08.029

2006; Pájaro et al., 2017), for which the stationary solution is also unique Cañizo et al. (2019).

In this work, we obtain and exploit the First Passage Times of proteins to quantify the robustness of the hysteresis effect. First Passage Times (FPT) also called hitting or escape times of proteins in gene regulatory circuits are defined as the times taken by a protein to reach some threshold or leave some region starting from a given initial state. In the literature, FPT have been used for example to explore the robustness of cellular memory or division (Cheng et al., 2008; Charlebois et al., 2011), the switching times between the two stable states (Zheng et al., 2011; Wang and Yang, 2016), the randomness on the timing of events (lytic pathway of the bacterial virus phage λ) Singh and Dennehy (2014), or to reduce the FPT noise Ghusinga et al. (2017).

Here, we derive the backward master equation with jump processes for gene self regulated networks to obtain the FPT distributions. We compute the mean FPT that is needed to attain the mean of the stationary protein distribution (given by the forward PIDE steady state solution) starting in absence of proteins. We show how the inverse of these times are in agreement with the convergence rates obtained by Pájaro et al. (2019) to measure the hysteresis strength. Moreover, hysteretic behaviour is more robust as the mean FPT to switch between the two most probable states increases.

In addition, we provide a theoretical basis to explain coexistence of different phenotypes, each of them characterized by a high probability region separated from neighbouring phenotypes by low probability barriers. Since we are far away from a thermodynamic limit, a potential-like characterization of phenotypes -the so-called Waddington landscape (see for instance Ferrell, 2012) - can be misleading as it suggests that under noise, some phenotypes are abandoned against others. Alternatively, we propose the use of the CME to construct a time evolving landscape in which phenotypes coexist rather than prevail at different levels of persistence.

2. METHODS

2.1 Model structure and assumptions

Let us consider the transcription-translation mechanism expressing a protein X depicted in Fig. 1. Transitions between inactive to active states (DNA_{off} and DNA_{on}, respectively) are regulated by a positive feedback mechanism which involves the binding of a given (positive) number $-H$ of protein molecules, and takes the form:

$$c(x) = (1 - \rho(x)) + \rho(x)\varepsilon, \tag{1}$$

where $\rho(x)$ is a Hill function that describes the ratio of promoter in the inactive form as a function of the number of proteins x:

$$\rho(x) = \frac{1}{1 + \left(\frac{x}{K}\right)^{-H}}. \tag{2}$$

with $K = \frac{k_{on}}{k_{off}}$ being the equilibrium binding constant and ε a small constant, typically much smaller than unity, which describes basal transcription (or leakage). Transcription and translation occur at rates k_m and k_x

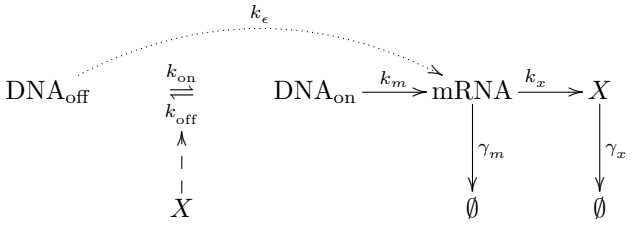

Fig. 1. Schematic diagram of a simple self-regulated protein expression network.The gene promoter is assumed to switch between an active and an inactive state denoted by DNA_{on} and DNA_{off} at frequencies k_{on} and k_{off}, respectively. Activation is exerted by a positive feed-back loop which consists of the binding of the expressed protein X. The loop is closed by a DNA to messenger RNA ($mRNA$) transcription and translation from $mRNA$ to protein.

per unit time, whereas γ_m and γ_x are degradation rate constants of mRNA and protein, respectively.

Assuming that $mRNA$ degrades faster than protein X as it is the case in most prokaryotic and eukaryote organisms (Dar et al., 2012), proteins are produced in bursts (Friedman et al., 2006; Ochab-Marcinek and Tabaka, 2015) at a frequency $a = k_m/\gamma_x$.

2.2 The forward Friedman equation

Under the previous assumption, let $p(x, t; x', t')$ be the probability of being in x at time t conditioned to be in x' at $t' \leq t$ (in what follows, t and t' are dimensionless). Then we have that $p(x, t; x', t')$ satisfies a Partial Integro-Differential Equation (PIDE) (Friedman et al., 2006; Pájaro et al., 2015) denoted here as forward Friedman equation. This equation is written only in terms of the variables t and x (t' and x' act as parameters) and takes the form:

$$\frac{\partial p(t,x)}{\partial t} - \frac{\partial [x p(t,x)]}{\partial x} = -ac(x)p(t,x) + a\int_0^x \mathrm{d}y\, \omega(x-y)c(y)p(t,y), \tag{3}$$

where $\omega(x - y)$ represents the conditional probability for protein number to jump from a state y to an upper state x after a burst of size $b = k_x/\gamma_m$, as follows:

$$\omega(x-y) = \frac{1}{b}\exp\left[\frac{-(x-y)}{b}\right]. \tag{4}$$

The solution of Eqn (3) requires as initial condition some initial probability distribution, typically of the form $p(x, 0) = \delta(x - x_0)$. In addition, we have that:

$$\int_0^\infty \mathrm{d}x\, p(x, t; x_0, 0) = 1, \tag{5}$$

where the equality must be satisfied for every positive time. The stationary solution of Eqn (3) is given by:

$$P(x) = Z\left(K^H + x^H\right)^{\frac{a(\varepsilon-1)}{H}} x^{a-1} e^{\frac{-x}{b}}, \tag{6}$$

with Z being the integration constant that normalizes the probability density function, $\int_0^\infty P(x)\,\mathrm{d}x = 1$, and the parameters H, K, ε, $a = \frac{k_m}{\gamma_x}$ and $b = \frac{k_x}{\gamma_m}$ being as in

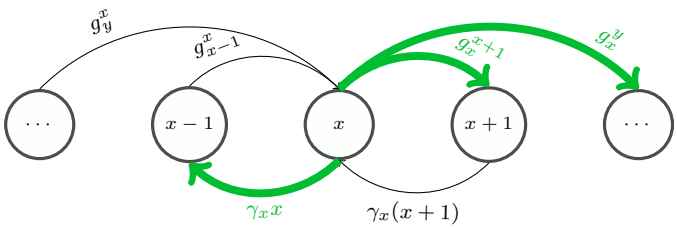

Fig. 2. Jump process representation of one protein produced in bursts, where one state x can be reached from lower states $0 \leq y < x$ with different transition probability functions g_y^x. Equivalently, from the state x the protein number can jump to higher states y with transition probability function g_x^y. The degradation follows a one step process (i. e. from state x to state $x-1$). The reactions highlighted in green, are the ones that appear in the First Passage Time (FPT) formula.

Eqn (3). Moreover, the dynamics of Eqn (3) are obtained by a semi-Lagrangian method (Pájaro et al. (2017)), implemented in the freely available toolbox SELANSI (Pájaro et al., 2018).

We can interpret the solution of Eqn (3) as a time evolving landscape with local maxima representing the set of coexisting phenotypes within a given isogenic cell population, and very unlikely cell states lying at the transition regions between most feasible phenotypes.

2.3 Backward master equations

In order to know for how long a particular phenotype can persist, we will be interested in computing first passage time distributions (e.g. Gardiner, 2009) associated to some given phenotype passing through a transition region characterized by a protein amount x_f. Such distributions can be obtained as follows:

$$\mathcal{T}(t) = \frac{q(x_f, t; x_0, 0)}{\int_0^T \mathrm{d}s\, q(x_f, s; x_0, 0)} \tag{7}$$

where T is chosen to be large enough, and $q(x', t'; x, t)$ (with $t' \geq t$) is a probability distribution function in x', that defines the probability of some given protein amount x' being produced in the future t', conditioned to a continuous set of possible values x produced in a given present t. Note that both x and x' lie within an interval (L, U) within the set of natural numbers. Moreover $x, x' \in (L, U)$.

We make use of the Chapman-Kolmogorov relation (see e.g. Gardiner (2009)) associated to our system, depicted in Figure 2, to compute the conditional probability $q(x', t'; x, t)$ as $t \to 0$. For every $x = L, \cdots, U$ we have:

$$\begin{aligned} q(x', t'; x, t) = {} & q(x', t'; x-1, t+\delta s)\gamma_x x \delta s \\ & + \sum_{y=x+1}^{\infty} q(x', t'; y, t+\delta s) g_x^y \delta s \\ & + q(x', t'; x, t)\left(1 - \gamma_x x \delta s - \sum_{y=x+1}^{\infty} g_x^y \delta s\right) \end{aligned} \tag{8}$$

with,

$$g_x^y = \frac{a}{b} c(x) e^{\frac{x-y}{b}}. \tag{9}$$

Re-ordering terms in the above equation (8) and dividing by δs we get the equivalent expression:

$$\begin{aligned} & \frac{q(x', t'; x, t) - q(x', t'; x, t+\delta s)}{\delta s} = \\ & q(x', t'; x-1, t+\delta s)\gamma_x x + \sum_{y=x+1}^{\infty} q(x', t'; y, t+\delta s) g_x^y \\ & \qquad - q(x', t'; x, t+\delta s)\left(\gamma_x x + \sum_{y=x+1}^{\infty} g_x^y\right) \end{aligned} \tag{10}$$

In the limit as $\delta s \to 0$, the left hand term of the above expression becomes a time derivative, leading to a set of ordinary differential equations (ODEs) for every $x = L, L+1, \cdots, U$, of the form:

$$\begin{aligned} -q_t(x', t'; x, t) = {} & q(x', t'; x-1, t)\gamma_x x \\ & + \sum_{y=x+1}^{\infty} q(x', t'; y, t) g_x^y \\ & - q(x', t'; x, t)\left(\gamma_x x + \sum_{y=x+1}^{\infty} g_x^y\right). \end{aligned} \tag{11}$$

The last equation requires to be solved a final condition $q(x', t'; x, t') = f(x')$, for every $x (= x') = L, \cdots, U$, and:

$$\sum_{x=L}^{U} f(x) = 1.$$

In what follows, we omit the explicit final condition in q considering that $q(x, t) \equiv q(x', t'; x, t)$. The final value problem just stated can be transformed into an equivalent initial value problem by using a new time variable $\tau = t' - t$, for t' large enough. Note that $q(x, \tau) = q(x, t)$ and $q_\tau(x, \tau) = -q_t(x, t)$, and therefore from Eqn (11) we obtain:

$$\begin{aligned} q_\tau(x, \tau) = {} & \gamma_x x q(x-1, \tau) + \sum_{y=x+1}^{\infty} g_x^y q(y, \tau) \\ & - \left(\gamma_x x + \sum_{y=x+1}^{\infty} g_x^y\right) q(x, \tau), \end{aligned} \tag{12}$$

which can be written in matrix notation as:

$$\boldsymbol{q}_\tau = \mathcal{F}\boldsymbol{q}, \tag{13}$$

where $\boldsymbol{q} \in \mathbb{R}^n$ (with $n = U - L + 1$) is a vector with elements being the values of $q(x, t)$ for each $x = L, L+1, \cdots, U$, such that $\boldsymbol{q} = [q(L, t), \cdots, q(U, t)]^T$, and the matrix $\mathcal{F} \in \mathbb{R}^{n \times n}$ in (13) reads:

$$\mathcal{F} = \begin{pmatrix} -d_L & g_L^{L+1} & g_L^{L+2} & \cdots & g_L^{U-2} & g_L^{U-1} & g_L^U \\ L+1 & -d_{L+1} & g_{L+1}^{L+2} & \cdots & g_{L+1}^{U-2} & g_{L+1}^{U-1} & g_{L+1}^U \\ 0 & L+2 & -d_{L+2} & & g_{L+2}^{U-2} & g_{L+2}^{U-1} & g_{L+2}^U \\ \vdots & & \ddots & \ddots & & \vdots & \vdots \\ 0 & 0 & 0 & & -d_{U-2} & g_{U-2}^{U-1} & g_{U-2}^U \\ 0 & 0 & 0 & & U-1 & -d_{U-1} & g_{U-1}^U \\ 0 & 0 & 0 & \cdots & 0 & U & -d_U \end{pmatrix}. \tag{14}$$

The elements of the diagonal d_i are of the form:

$$d_L = \sum_{i=L+1}^{\infty} g_L^i = \frac{a}{b}\frac{c(L)}{e^{\frac{1}{b}}-1}, \tag{15}$$

and

$$d_n = n + \sum_{i=n+1}^{\infty} g_n^i = n + \frac{a}{b}\frac{c(n)}{e^{\frac{1}{b}}-1}, \tag{16}$$

for $n = L+1, L+2, \ldots, U$. The set of ODEs in (13) is solved directly using matrix exponentiation in MATLAB. Note that $\mathcal{F}$ is equivalent to the transpose of the matrix associated to the forward PIDE, $\mathcal{M}^T$, see Pájaro et al. (2019). The only difference between both matrices appears in the diagonal terms which have been truncated for the forward problem, whereas for the backward one, infinite jump terms were considered.

Moreover, from Eqn (11) we can obtain its continuous counterpart, denoted here as backwards in time PIDE, which reads:

$$\frac{\partial q(x,t)}{\partial t} - x\frac{\partial [q(x,t)]}{\partial x} = \\ +ac(x)q(x,t) - ac(x)\int_x^{\infty} \mathrm{d}y\, \omega(x-y)q(y,t). \tag{17}$$

The above backwards in time PIDE must satisfy a final value condition of the form $q(x_f, T) = \delta(x - x_f)$ that represents some certainty of being in x_f in the future. Eqn (17) can be solved by a semi-Lagrangian method (Pájaro et al. (2018)) in the same way as Eqn (3), transforming the backward Friedman equation into an initial value problem by reverting time such that $\tau = T - t$.

The mean FPT, $\langle T \rangle$ is obtained by computing the mean of the FPT distributions, $\mathcal{T}(t)$ in Eqn 8. The mean FPT of going from zero proteins to a certain positive threshold, x_f, can be also computed as the mean FPT of exit from the region $[0, x_f]$. Note that, zero is a natural boundary of the system (we cannot have negative amounts of proteins), so that, x_f is the unique point to escape from the region. Following Van Kampen (2007), the mean FPT of exit from one region is defined as:

$$T(x) = \mathrm{d}t + \mathrm{d}t \sum_{i=x+1}^{\infty} g_x^i T(i) + \mathrm{d}t x T(x-1) \\ + T(x)\left(1 - \mathrm{d}t x - \mathrm{d}t \sum_{i=x+1}^{\infty} g_x^i\right). \tag{18}$$

Considering the limit $\mathrm{d}t \to 0$, the above expression takes the following form:

$$-1 = \sum_{i=x+1}^{\infty} g_x^i T(i) + xT(x-1) - \left(x + \sum_{i=x+1}^{\infty} g_x^i\right) T(x). \tag{19}$$

Note that, Eqn (19) can be also written in matrix notation as:

$$-\mathbf{1} = \mathcal{F}\boldsymbol{T}, \tag{20}$$

where $\boldsymbol{T} \in \mathbb{R}^n$ (with $n = U - L + 1$) is a vector with elements being the values of $T(x)$ for each $x = L, L+1, \cdots, U$, and $\mathcal{F}$ as defined in (14). Eqn (20) can be directly solved by computing the matrix inverse, $\boldsymbol{T} = -\mathcal{F}^{-1}\mathbf{1}$. Thus the mean FPT for reach U proteins from zero is $\langle T \rangle = \boldsymbol{T}(1)$.

3. RESULTS AND DISCUSSION

As discussed in the introduction, despite the number of experimental and theoretical works supporting evidence of hysteresis in GRN, such phenomenon is not compatible with the stochasticity underlying gene regulatory networks dynamics. At least, not in the conditions that typically characterize hysteresis in systems operating in the thermodynamic/deterministic limit. It is a well known fact that any CME (Chemical Master Equation) has a unique (and stable) equilibrium solution (Van Kampen, 2007). According to Cañizo et al. (2019), this is the case also for the PIDE approximation of the CME in Eqn (3).

In a previous work (Pájaro et al., 2019) we found that within slow transients of Eqn (3), mean protein values relate to kinetic parameters by a typical hysteresis pattern as the one depicted in Figure 3 A as a function of parameter b. As the transient distributions starting from different initial conditions approach the steady state, hysteresis shrinks to actually collapse into the mean values of the steady state distribution (black line in Figure 3 A). Here we show how through the FPT derived in the Methods section, we can quantify the robustness of the hysteresis effect.

As in Pájaro et al. (2019), we compute the convergence rate, η, of the PIDE model, Eqn (3), for different initial conditions (blue and red lines in Figure 3 B) and the eigenvalue with smallest absolute value of $\mathcal{M}$ associated to Eqn (3), λ_1, (black line in Figure 3 B). In addition, we plot the mean FPT to reach the mean protein level (obtained from the analytical expression (6)) starting from zero. The inverse of that mean FPT is shown in Figure 3 B (magenta dashed line), which follows the same trajectory than the convergence rate obtained for initial condition close to zero (a normal distribution centered at 1, $\mathcal{N}(1, 0.1)$). Higher values of the mean FPT are obtained for b parameters for which the hysteresis behaviour is more persistent.

Regions in the a-b parameter space leading to bimodal distributions Pájaro et al. (2015), coincide with those for which Eqn (3) evolves slowly and the mean FPT is higher. Figure 3 C depicts one such region characterized by the mean FPT, $\langle T \rangle$, to reach the mean protein amount from zero computed using expression (20) (in the figure the logarithm is plotted).

Typical (bimodal) stationary distributions are presented in Figure 4 A. Extremal values of bimodal distributions are often related to multiple equilibria of the corresponding deterministic description, being the maxima and the minimum associated to stable and unstable equilibria, respectively. Unfortunately, this correspondence fails in many occasions, so that bimodal distributions associated to a mesoscopic description do not necessarily coincide with bistable states of the deterministic counterpart, or the other way around Pájaro et al. (2015). This calls for a mesoscopic (CME-type) framework to be the more adequate and natural representation of the gene regulatory phenomena.

In this context, the number of possible phenotypes that can be reached by a cell should equal the number of maxima in $p(x,t)$, each of them is characterized by a high probability region separated from neighbouring phenotypes by low probability barriers. Since the systems under study

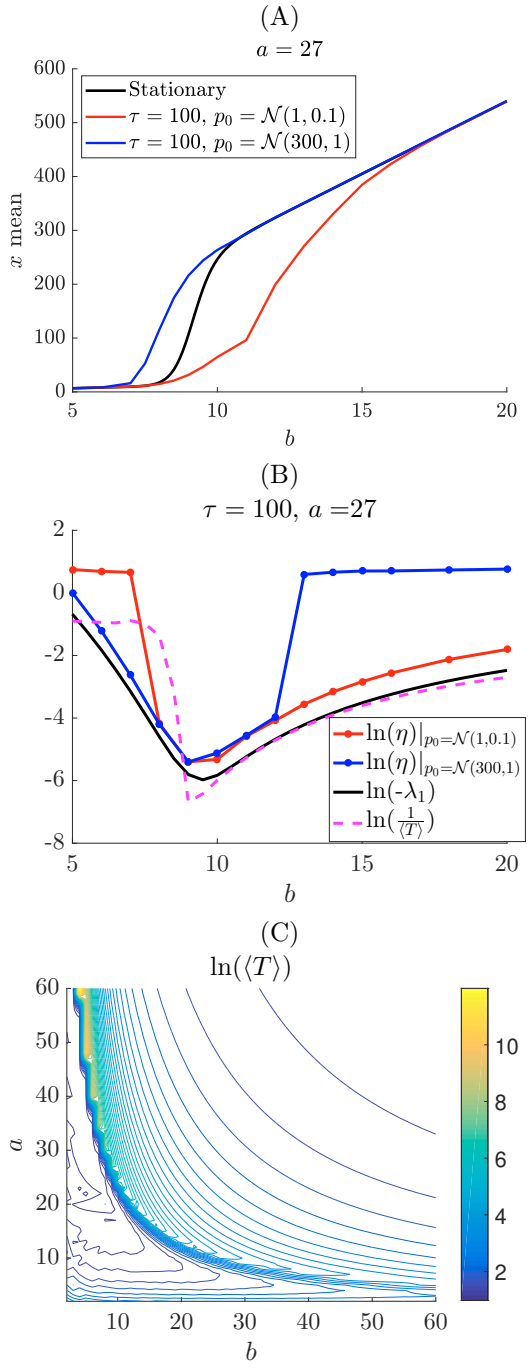

Fig. 3. Transient hysteresis in a self-regulating network with $H = -7$, $K = 100$. Plot (A) compares mean values of x obtained from different initial conditions p_0 at $t = 100$ (dimensionless time units) with the values obtained for the stationary distribution, for different b values. Parameter $a = 27$. Plot (B) shows the convergence rates, η of Eqn (3) for different initial conditions, the slowest (negative) eigenvalue associated to Eqn (3) and the mean FPT to reach the mean protein amount from zero. Plot (C) represents mean FPT to reach the mean protein amount from zero as a function of the burst frequency and size, a and b parameters, respectively.

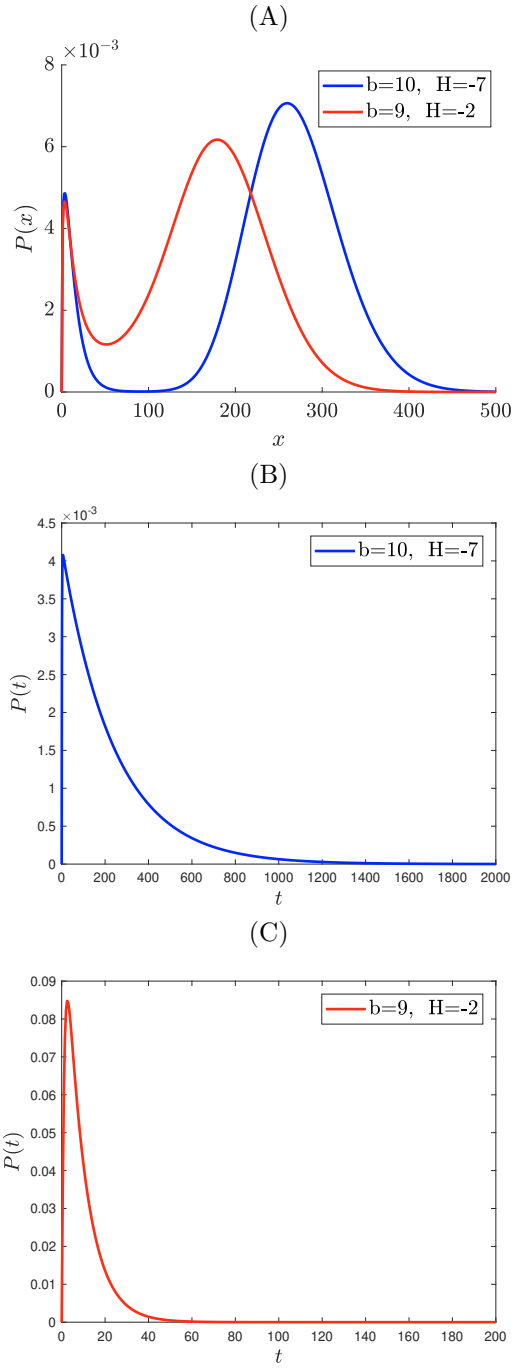

Fig. 4. A positive self-regulating network with $K = 100$ and $a = 27$. (A) represents stationary distributions for $b = 10$, $H = -7$ (blue line) and $b = 9$, $H = -2$ (red line). (B) and (C) are first passage time distributions for the low protein expression phenotype, computed from Eqn (7) for the cases shown above. (B) distribution for $b = 10$, $H = -7$, (C) distribution for $b = 9$, $H = -2$.

are far from the thermodynamic limit, we make use of the CME (in our case approximated through the forward Friedman Eqn (3)) to provide a description based on a time evolving landscape where phenotypes can coexist, being more or less persistent, rather than stable or unstable.

Figure 4 B-C depicts the first passage time distributions computed from (7) and (13). Comparing both distributions with those of Figure 4 A, the less probable the separation between phenotypes, the longer the first passage times. In agreement with this observation, the slower the forward Friedman equation as well, even to the point of such solution being confounded by a stationary one.

The above results suggests the use of the mean first passage times (or first passage time distributions) as a measure of phenotype persistency, a concept that would substitute the notion of stability, more appropriate for deterministic systems governed by a potential.

REFERENCES

Cañizo, J.A., Carrillo, J.A., and Pájaro, M. (2019). Exponential equilibration of genetic circuits using entropy methods. *J. Math. Biol.*, 78, 373–411.

Celià-Terrassa, T., Bastian, C., Liu, D., Ell, B., Aiello, N.M., Wei, Y., Zamalloa, J., Blanco, A.M., Hang, X., Kunisky, D., Li, W., Williams, E.D., Rabitz, H., and Kang, Y. (2018). Hysteresis control of epithelial-mesenchymal transition dynamics conveys a distinct program with enhanced metastatic ability. *Nature Communications*, 9(1), 5005.

Charlebois, D.A., Abdennur, N., and Kaern, M. (2011). Gene expression noise facilitates adaptation and drug resistance independently of mutation. *Physical Review Letters*, 107(21), 218101.

Cheng, Z., Liu, F., Zhang, X.., and Wang, W. (2008). Robustness analysis of cellular memory in an autoactivating positive feedback system. *FEBS letters*, 582(27), 3776–3782.

Dar, R.D., Razooky, B.S., Singh, A., Trimeloni, T.V., McCollum, J.M., Cox, C.D., Simpson, M.L., and Weinberger, L.S. (2012). Transcriptional burst frequency and burst size are equally modulated across the human genome. *Proc. Natl. Acad. Sci. U.S.A.*, 109(43), 17454–17459.

Ferrell, J. (2012). Bistability, bifurcations, and waddington's epigenetic landscape. *Nature*, 22(11), R458–R466.

Friedman, N., Cai, L., and Xie, X.S. (2006). Linking stochastic dynamics to population distribution: An analytical framework of gene expression. *Phys. Rev. Lett.*, 97(16), 168302.

Gardiner, C. (2009). *Stochastic Methods. A Handbook for the Natural and Social Sciences*. Springer, Berlin, fourth edition.

Ghusinga, K.R., Dennehy, J.J., and Singh, A. (2017). First-passage time approach to controlling noise in the timing of intracellular events. *Proceedings of the National Academy of Sciences of the United States of America*, 114(4), 693–698.

Gnügge, R., Dharmarajan, L., Lang, M., and Stelling, J. (2016). An Orthogonal Permease–Inducer–Repressor Feedback Loop Shows Bistability. *ACS Synth. Biol.*, 5, 1098–1107.

Gupta, P., Fillmore, C., Jiang, G., S.D., S., Tao, K., Kuperwasser, C., and E.S., L. (2011). Stochastic state transitions give rise to phenotypic equilibrium in populations of cancer cells. *Cell*, 146(4), 633–644.

Hsu, C., Jaquet, V., Gencoglu, M., and Becskei, A. (2016). Protein Dimerization Generates Bistability in Positive Feedback Loops. *Cell Reports*, 16(5), 1204–1210.

Ochab-Marcinek, A. and Tabaka, M. (2015). Transcriptional leakage versus noise: A simple mechanism of conversion between binary and graded response in autoregulated genes. *Phys. Rev. E*, 91(1), 012704.

Ozbudak, E., Thattai, M., Lim, H., Shraiman, B., and van Oudenaarden, A. (2008). Multistability in the lactose utilization network of *Escherichia coli*. *Nature*, 427, 737–740.

Pájaro, M., Alonso, A.A., Otero-Muras, I., and Vázquez, C. (2017). Stochastic modeling and numerical simulation of gene regulatory networks with protein bursting. *J. Theor. Biol.*, 421, 51–70.

Pájaro, M., Alonso, A.A., and Vázquez, C. (2015). Shaping protein distributions in stochastic self-regulated gene expression networks. *Phys. Rev. E*, 92(3), 032712.

Pájaro, M., Otero-Muras, I., Vázquez, C., and Alonso, A.A. (2018). SELANSI: a toolbox for Simulation of Stochastic Gene Regulatory Networks. *Bioinformatics*, 34(5), 893–895.

Pájaro, M., Otero-Muras, I., Vázquez, C., and Alonso, A.A. (2019). Transient hysteresis and inherent stochasticity in gene regulatory networks. *Nature Communications*, 10(1).

Singh, A. and Dennehy, J.J. (2014). Stochastic holin expression can account for lysis time variation in the bacteriophage λ. *Journal of the Royal Society Interface*, 11(95), 20140140.

Thomas, P., Popovic, N., and Grima, R. (2014). Phenotypic switching in gene regulatory networks. *Proceedings of the National Academy of Sciences USA*, 111(19), 6994–6999.

Van Kampen, N.G. (2007). *Stochastic Processes in Physics and Chemistry*. Elsevier, Netherlands, third edition.

Veening, J., Smits, W., , and Kuipers, O. (2008). Bistability, epigenetics and bet-hedging in bacteria. *Annu. Rev. Microbiol.*, 62, 193–210.

Wang, C.. and Yang, K.. (2016). Correlated noise-based switches and stochastic resonance in a bistable genetic regulation system. *European Physical Journal B*, 89(8), 173.

Wang, L., Walker, B., Iannaccone, S., Bhatt, D., Kennedy, P.J., and Tse, W.T. (2009). Bistable switches control memory and plasticity in cellular differentiation. *Proc. Natl. Acad. Sci. U.S.A.*, 106(16), 6638–6643.

Wu, M., Su, R., Li, X., Ellis, T., Lai, Y., and Wang, X. (2013). Engineering of regulated stochastic cell fate determination. *Proc. Natl. Acad. Sci. U.S.A.*, 110(26), 10610–10615.

Xiong, W. and Ferrell, J. (2012). A positive-feedback-based bistable 'memory module' that governs a cell fate decision. *Nature*, 426, 460–465.

Zheng, X.., Yang, X.., and Tao, Y. (2011). Bistability, probability transition rate and first-passage time in an autoactivating positive-feedback loop. *PLoS ONE*, 6(3), e17104.